ELSEVIER Nuclear Instruments and Methods in Physics Research B 148 (1999) 1102–1105

NIM B
Beam Interactions
with Materials & Atoms

Carbon nanotubes produced by high energy ($E > 100$ MeV), heavy ion irradiation of graphite

L.P. Biró [a,*], B. Szabó [a], G.I. Márk [a], J. Gyulai [a], K. Havancsák [b], J. Kürti [c], A. Dunlop [d], L. Frey [e], H. Ryssel [e]

[a] *Research Institute for Technical Physics and Materials Science, H-1525 Budapest, P.O. Box 49, Hungary*
[b] *Eötvös University, Institute for Solid State Physics, H-1088 Budapest, Múzeum krt.6-8, Hungary*
[c] *Eötvös University, Department of Biological Physics, H-1088, Puskin u. 5-7, Hungary*
[d] *CEA/DTA/CEREM/DTM, Laboratoire des Solides Irradies, Ecole Polytechnique, 91128 Palaiseau Cedex, France*
[e] *FhG-Institut für Integrierte Schaltungen IIS-B, 91058 Erlangen, Schottkystr.10, Germany*

Abstract

Scanning tunneling microscopy (STM) and atomic force microscopy (AFM) were used to investigate the surface of highly oriented pyrolytic graphite (HOPG) irradiated with 209 MeV Kr or 830 MeV U ions. The density of hillocks found on samples irradiated by Kr and U ions indicates synergism of electronic and nuclear stopping processes. Carbon nanotubes (CNTs) were found on all of the investigated samples, STM images show an atomic arrangement identical with that of graphite. AFM revealed sputtering craters from which emerge CNTs, the vibration of some CNTs was observed. © 1999 Elsevier Science B.V. All rights reserved.

PACS: 61.48.+c; 61.16.Ch; 61.80.Jh; 81.05.Ys; 85.40.Ux
Keywords: Carbon nanotubes (CNTs); STM; AFM; Ion irradiation; Atomic resolution on carbon nanotubes

1. Introduction

Carbon nanotubes (CNTs) are a new allotrope member of the fullerene family [1]. Iijima [2] discovered these objects in 1991 by electron microscopy in electric arc soot. A single wall CNT is constituted of one atomic sheet with a graphite-like arrangement of C atoms – called graphene sheet – rolled into a cylinder. Tube diameters are in the 1 nm range. Multi-wall CNTs are built of several coaxial layers of graphene cylinders with an interlayer spacing of 0.34 nm. External diameters are of several tens to hundreds of nm. Remarkable electronic and mechanical properties put CNTs in the focus of recent research. Most important theoretical and experimental results have been summarized in Refs. [3,4]. CNTs may have metallic or semiconducting behavior depending on the way the graphene is rolled to form the tube. Recent papers report good agreement between theoretical gap values and STS measurements on single wall CNTs [5,6].

---

[*] Corresponding author. Tel.: +36 1 3959220; fax: +36 1 3959284; e-mail: biro@mfa.kfki.hu

PII: S0168-583X(98)00738-1

Three methods are widely used for the production of CNTs: the electric arc method [7], the laser ablation method [8], and variations of the catalytic method [9]. Although the growth mechanism of the CNTs is not yet clear, in all three methods an atmosphere of excited carbon atoms is produced, from which the condensation of CNTs takes place.

The production of CNTs by 10^{18} cm^{-2}, 3 keV Ar ion irradiation of amorphous carbon was reported [10]. Recently, we reported the observation of CNTs on HOPG irradiated with low dose, high energy ($E > 100$ MeV) Ne, Kr, and Xe ions [11]. In the present paper, we report results for HOPG targets irradiated with 830 MeV U ions and we compare these results with those obtained with 209 MeV Kr ions.

2. Experimental results and discussions

Freshly cleaved HOPG was irradiated under normal incidence with 10^{12} cm^{-2} 209 MeV Kr, or with 10^{12} cm^{-2} 830 MeV U ions. Sample evaluation was done in air by STM and tapping mode (TM) AFM. Mechanically prepared Pt–Ir STM tips, and etched single crystalline Si AFM tips were used.

The most frequently found features were the well-known hillocks [12], attributed to nuclear stopping effects. The relative densities of hillocks, i.e., the ratio of the surface density of hillocks to the ion dose was of the order of 10^{-2} for Kr and 0.5 for U irradiation. The ratios of stopping powers at the incidence energy are $R_n = [(\mathrm{d}E/\mathrm{d}x)_n{}^{\mathrm{U}}]/[(\mathrm{d}E/\mathrm{d}x)_n{}^{\mathrm{Kr}}] = 4.23$ and $R_e = [(\mathrm{d}E/\mathrm{d}x)_e{}^{\mathrm{U}}]/[(\mathrm{d}E/\mathrm{d}x)_e{}^{\mathrm{Kr}}] = 2.47$. Velocities of the two incoming ions are $v_{\mathrm{U}} = 2.5\times10^7$ m/s, and $v_{\mathrm{Kr}} = 2.1\times10^7$ m/s. R_n shows that the difference of nuclear stopping powers by itself cannot explain the difference in relative densities of the hillocks. Therefore, some synergistic interaction of the electronic and nuclear stopping powers has to be involved. An STM image which supports this idea is shown in Fig. 1. The two straight, linear features which make an angle of 1.5° are attributed to a high energy, knocked on target particle moving one atomic plane below the surface. In the region where the two straight lines would come to crossing a large area defect with irregular shape is seen. The height of the linear feature as measured in the section labeled 1 is 3.4 Å, while the depth of the defect measured in section 2 is 3.4 Å, i.e., one atomic layer is missing. The change in the direction of the trajectory and the large area, irregular surface defect, both indicate nuclear collision. A simple, binary collision with a target atom hardly could generate such an extended defect. The straight linear features before and after the collision indicate the dominance of electronic stopping. The size of the defect may be explained by a synergistic interaction of the electronic and nuclear stopping mechanisms. Results indicating synergism of the two stopping mechanisms in defect production have been reported earlier [13–15].

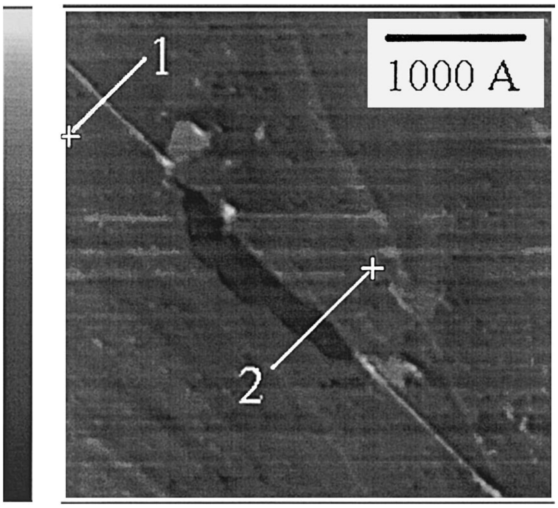

Fig. 1. Constant current STM image of HOPG irradiated with 830 MeV U ions, the gray scale corresponds to a vertical height of 11.7 Å. The two, white linear features from the upper left to the lower right corner are tracks of a high energy particle.

CNTs were observed both on the samples irradiated with Kr or U ions. In Fig. 2, an individual CNT is seen on Kr-irradiated HOPG, which crosses a 3 atomic layer high step. The apparent height of the CNT is 4 Å. This is an underestimated value due to differences in the electronic structure of the CNT and that of HOPG [16]. On the samples irradiated with U ions, several bundles of CNTs were found, like the ones shown in Fig. 3.

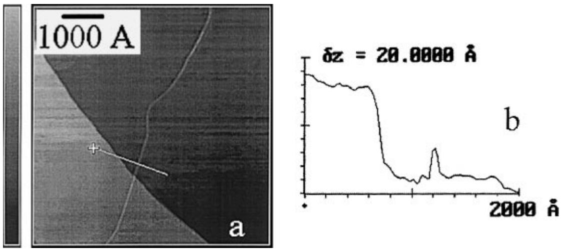

Fig. 2. Constant current STM image of HOPG irradiated with 209 MeV Kr ions. A CNT is crossing a cleavage step of 3 atomic layers height. The grey scale corresponds to 27 Å. The line cut taken along the white line in (a) is shown in (b).

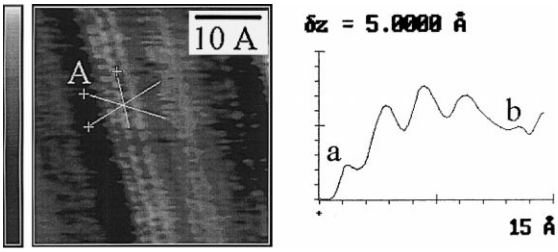

Fig. 4. Atomic resolution STM image on a CNT from the bundle in Fig. 3; the grey scale corresponds to 6.8 Å. The white lines indicate the axes along which the periodic arrangement of tunneling maxima is found. The line cut along line A is shown on the right side.

In some cases atomic resolution was achieved on CNTs in the bundle, Fig. 4. The three axes along which periodic arrangement of the maxima is found are marked by white lines in the image. Along the line labeled *A*, a periodicity of 2.43 Å is measured between the topmost maxima of the line cut, in good agreement with the periodicity of HOPG and of CNTs [16].

TM AFM investigation of samples irradiated with Kr or Xe ions evidenced craters with typical diameters in the μm range and depths of some tens of nm [11]. Similar features were found on the HOPG targets irradiated with U ions. Frequently, from these craters emerge one or several multi-wall CNTs with lengths of the order of 10 μm. We attribute the craters to extensive surface sputtering produced by dense nuclear cascades which propagate from the bulk towards the irradiated surface, similarly to those on muscovite mica reported earlier [14] (Fig. 4 in Ref. [14]). The ratio of the surface density of the craters observed on HOPG to the Kr dose used is 10^{-7}; 5% of the material missing from the crater is present as CNTs [11].

When scanned by the TM AFM, some CNTs which cross elevated surface features, like the one in Fig. 5, show a regular vibration pattern. In Fig. 5, the CNT crosses a surface fold, which was produced during the cleavage of the sample. The shape of the object identified with a CNT climbing and descending the fold, clearly shows that the object is different from that kind of surface modification which is produced along the trajectory of an energetic particle, see Fig. 1. A CNT like in Fig. 5 can grow in the expanding cloud of C atoms and clusters sputtered from the crater [11]. After the quick growth stage, the CNT collapses onto the surface of the target. There, additional growth may take place due to the incorporation of low energy C atoms diffusing on the surface, which

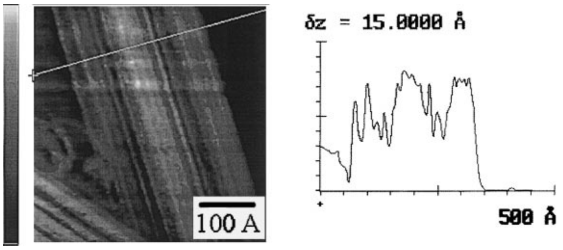

Fig. 3. STM image of crossing bundles of CNTs on HOPG irradiated with 830 MeV U ions, the grey scale corresponds to 15.1 Å. The diameters of the CNTs are in the 10 Å range.

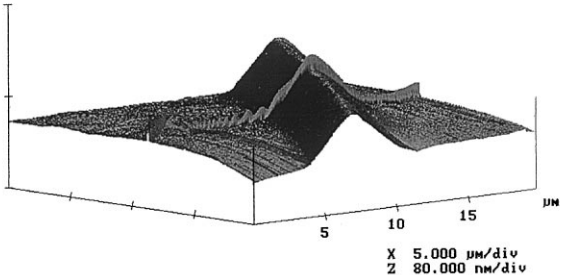

Fig. 5. Tapping mode AFM image of a vibrating CNT crossing a surface fold on HOPG irradiated with 209 MeV Kr ions.

were generated in those nuclear collisions which are responsible for the production of hillocks.

3. Conclusions

The surface density of hillocks as measured by STM on graphite targets irradiated with 209 MeV Kr or 830 MeV U ions indicates a synergistic interaction of electronic and nuclear stopping mechanisms. STM images of large area surface defects in association with linear features produced by electronic stopping effects come to support this idea.

CNTs were found on the samples irradiated with Kr, or U ions. Kr irradiation yielded only individual CNTs, while in the case of U irradiation bundles of CNTs were found, too. Atomic resolution was achieved on some of the CNTs in the bundles. A similar atomic arrangement as for graphite, or CNTs produced by other procedures was found.

AFM revealed sputtering craters on the irradiated surface of the targets, frequently, from these craters emerge CNTs. Those CNTs which cross elevated surface features, like folds, or cleavage steps, frequently vibrate when scanned by the AFM tip.

Acknowledgements

The authors wish to thank Dr. Cs. S. Daróczi for technical assistance. This work was supported by OTKA T017344 and T025928, AKP 96/2-637 and 96/2-462 grants.

References

[1] H.W. Kroto, J.R. Heath, S.C. O'Brien, R.F. Curl, R.E. Smalley, Nature 318 (1985) 162.
[2] S. Iijima, Nature 354 (1991) 56.
[3] M.S. Dresselhaus, G. Dresselhaus, P.C. Eklund, Science of Fullerenes and Carbon Nanotubes, Academic Press, San Diego, 1996.
[4] Th.W. Ebbesen (Ed.), Carbon CNTs Preparation and Properties, CRC Press, Boca Raton, 1997.
[5] J.W.G. Wildöer, L.C. Venema, A.G. Rinzler, R.E. Smalley, C. Dekker, Nature 391 (1998) 59.
[6] T.W. Odom, J.-L. Huang, Ph. Kim, Ch.M. Lieber, Nature 391 (1998) 62.
[7] T.W. Ebbesen, H. Hiura, J. Fujita, S. Ochiai, S. Matsui, K. Tanigaki, Chem. Phys. Lett. 209 (1993) 83.
[8] A. Thess, R. Lee, P. Nikolaev, H. Dai, P. Petit, J. Robert, C. Xu, Y.H. Lee, S.G. Kim, A.G. Rinzler, D.T. Colbert, G.E. Scuseria, D. Tománek, J.E. Fischer, R.E. Smalley, Science 273 (1996) 483.
[9] V. Ivanov, J.B. Nagy, Ph. Lambin, A. Lucas, X.B. Zhang, X.F. Zhang, D. Bernaerts, G. Van Tendeloo, S. Amelinckx, J. Van Ladyst, Chem. Phys. Lett. 223 (1994) 329.
[10] K. Yamamoto, Y. Koga, S. Fujiwara, M. Kubota, Appl. Phys. Lett. 69 (1996) 4174.
[11] L.P. Biró, G.I. Márk, J. Gyulai, K. Havancsák, S. Lipp, Ch. Lehrer, L. Frey, H. Ryssel, Proc. European Materials Research Society Spring Meeting, Symposium J, 1998 Nucl. Instr. and Meth. B 147 (1999) 142.
[12] T. Li, B.V. King, R.J. MacDonald, G.F. Cortelli, D.J. O'Connor, Q. Yang, Surf. Sci. 312 (1994) 399.
[13] V.S. Varichenko, A.M. Zaitsev, N.M. Kazutchis, A.R. Chelyadinskii, N.M. Penima, V.A. Martinovich, Ya.I. Latuskho, W.R. Fahrner, Nucl. Instr. and Meth. B 107 (1996) 268.
[14] L.P. Biró, J. Gyulai, K. Havancsák, Vacuum 50 (1998) 263.
[15] T. Schenkel, A.V. Barnes, A.V. Hazma, D.H. Scheider, J.C. Banks, B.L. Doyle, Phys. Rev. Lett. 80 (1998) 4325.
[16] L.P. Biró, J. Gyulai, Ph. Lambin, J.B. Nagy, S. Lazarescu, G.I. Márk, A. Fonseca, P.R. Surján, Zs. Szekeres, P.A. Thiry, A.A. Lucas, Carbon 36 (1998) 689.